Visible/Near-Infrared Spectra and Two-Layer Modeling of Palagonite-Coated Basalts

Jeffrey R. Johnson
U.S. Geological Survey, Flagstaff, AZ 86001

William M. Grundy
Lowell Observatory, Flagstaff, AZ 86001

Abstract. Fine-grained dust coatings on Martian rocks and soils obscure underlying surfaces and hinder mineralogic interpretations of both remote sensing and in-situ observations. We investigate laboratory visible/near-infrared spectra of various thicknesses of palagonite coatings on basalt substrates. We develop a two-layer Hapke scattering model incorporating porosity, grain size, and derived absorption coefficients of palagonite and basalt that reproduces the observed spectra only when the single scattering particle phase function is varied with wavelength.

Introduction

Surface albedo variations associated with the aeolian deposition and erosion of dust (i.e., <40 μm particles) on Mars have been observed historically via ground-based telescopes (e.g., *Martin and Zurek, 1993*), Mariner and Viking orbital imaging (e.g., *Thomas et al., 1984; Arvidson et al., 1989a; Greeley et al., 1992*), Hubble Space Telescope imaging (e.g., *James et al., 1999; Bell et al., 1999*), and in Mars Observer Camera images (e.g., *Thomas et al., 1999*). *Christensen (1986)* concluded that global dust storms could deposit as much as ~ 250 μm per year in the equatorial region. The masking effects of such windblown and airfall-deposited dust on underlying rocks and soils hinders interpretations of reflectance and emission spectra of the surface obtained from orbit (*Mustard and Sunshine, 1995; Mustard et al., 1993; Christensen et al., 1992, 1998, 2000*) and from the Viking and Mars Pathfinder landers (*Arvidson et al., 1989b; McSween et al., 1999; Bell et al., 2000*). Dust coatings also hampered analyses of alpha proton x-ray (APXS) measurements of rocks (*Rieder et al., 1997; Crisp, 1998; McSween et al. 1999*) and decreased Sojourner rover solar panel power at the Mars Pathfinder site (*Landis and Jenkins, 2000*).

It is difficult to discriminate spectral features related to fine-grained coatings from those attributable to the underlying rock or soil, particularly when compensating for the effects of a dusty atmosphere with spectral features similar to surficial dust (*Pollack et al., 1979; Clancy et al., 1995; Tomasko et al., 1999*). Previous remote sensing work has relied on comparisons between "clean" and variously weathered or dust-coated regions to understand and attempt to compensate for the spectral effects of dust coatings (e.g., *Mustard and Sunshine, 1995*). Laboratory and field investigations of the spectral effects of dust and rock coatings have shown that thin (<100 μm) layers of such coatings can effectively mask the spectral signature of the underlying materials in both the visible/near-infrared and thermal infrared wavelengths (*Roush, 1982; Singer and Roush, 1983; Wells et al.,*

1984; Fischer and Pieters, 1993; Crisp and Bartholomew, 1992; Johnson et al., 1998). We investigate here the spectral effects of varying thicknesses of the Mars regolith simulant JSC-1 deposited onto basalt substrates and model the results using a two-layer Hapke radiative transfer model (*Hapke, 1993*).

Previous visible/near-infrared laboratory investigations of the spectral effects of dust coatings used variable methods of deposition and thickness measurement. *Singer and Roush (1983)* deposited palagonitic soil onto a basalt substrate using differential settling in a methanol suspension, and measured the coating thickness using thin sections of epoxy-coated samples. *Wells et al. (1984)* and *Thomas et al. (1984)* deposited fine-grained (<5 μm) palagonitic soil onto larger size-fractions of volcanic soil and basalt powders using an enclosed cylinder in which the palagonite particles settled onto the samples after being elevated by blasts of compressed air. By estimating the coating density and calculating its mass per unit area, they computed a coating thickness. *Fischer and Pieters (1993)* and *Hiroi and Pieters (1992)* deposited powders (<25 μm) onto a basaltic substrate using the differential settling method in ethanol and measured coating thickness directly using a calibrated microscope. None of these studies attempted to model quantitatively the effects of coatings. However, the usual observation of a negative spectral slope in the near-infrared of coated samples was typically explained by the increasing transparency of the coatings at longer wavelengths, resulting in a greater contribution from the substrate.

Methodology

A sample of fine-grained basaltic andesite (SP Flow, AZ) was cored, cut to provide 3.8 cm diameter disks, and polished using 400-grit to provide a surface roughness of ~22 μm. To mimic the aeolian deposition of dust onto rocks on Mars, a simple airfall deposition technique was used in which JSC-1 Mars analog soil (wet-sieved to <45 μm) was elevated by a pulse of compressed air and allowed to settle onto the substrate within an enclosed bell jar (cf. *Wells et al., 1984; Johnson et al., 2000*). JSC-1 soil is composed of Hawaiian palagonite (a poorly crystalline to amorphous basaltic weathering product) with many spectroscopic and physical properties similar to those observed for Martian soils (*Allen et al., 1998*). Average coating thicknesses were determined using a vertically calibrated microscope to measure the focus distances between the substrate and the coating at 25 locations on the coated sample. Nine coatings were acquired (cf. *Johnson et al., 2000*) of which three are presented here: 27 ± 11 μm, 53 ± 26 μm, and 106 ± 34 μm (Figure 1). The relatively high standard deviations were mainly due to the clumping of small particles into aggregates (~10-50 μm) during deposition (cf. *Crisp and Bartholomew, 1992*).

Reflectance spectra of the basalt, JSC-1 coating material, and coated samples were acquired using a FieldSpecFR (Analytical Spectral Devices, Inc., ASD) fiberoptic spectrometer operating over the 350-2500 nm wavelength range. The fiberoptic cable was interfaced with a cylindrical casing containing a quartz halogen light source that was placed directly over the sample and provided a 3 cm field-of-view. This allowed direct illumination (incidence angle=0º) and collection (emission angle=27º) of a sample spectrum, followed closely in time by acquisition of the spectrum of a white Spectralon (sintered halon) reflectance

standard panel. The near-Lambertian nature of Spectralon provided a suitable standard, particularly for this geometry. Dark current measurements were obtained before each spectrum acquisition, and twenty scans were averaged for each spectrum. Each sample spectrum was divided by the Spectralon spectrum, and the result was multiplied by the absolute reflectance spectrum of Spectralon (*Salisbury, 1998)*, followed by scaling to bidirectional reflectance (*Hapke, 1993*). Offsets between ASD detectors were corrected by performing a standard multiplicative scaling of both the first (350-980 nm) and third (1800-2500 nm) detector regions to the second detector region (980-1800 nm).

We next sought to model the complete data set with Hapke's multiple scattering radiative transfer model (*Hapke, 1993*), which has the advantages of being computationally inexpensive to evaluate and widely accepted for use in remote sensing applications. We used a two-layer version of the model (*Hapke, 1993, section 9.D.3*) to compute bidirectional reflectance for a geometry comparable to the observations as a function of the Hapke parameters w (single-scattering albedo), B_0 (opposition peak amplitude), h (opposition peak width), porosity, grain size, and single-scattering phase function $P(g)$. Because the opposition peak (zero phase angle) was not measured by our experimental configuration, we turned off the backscattering portion of the model by setting B_0 to zero. The only parameters dependent on wavelength (λ) are w and $P(g)$. We assumed $P(g)=1$ (isotropic single scattering) and used the standard Hapke equivalent-slab model to relate w to the grain size and optical constants α and n, as well as the internal scattering coefficient s, which we assumed to be zero. The refractive index n for JSC-1 was determined by a linear fit to the palagonite data (n=1.56084–0.052355*λ) from *Clark et al. (1990)*. For the basalt we assumed n=1.7. The value of n only enters into Hapke's model through w, which is much more strongly dependent on the imaginary part of the refractive index ($k=\alpha\lambda/4\pi$) than it is on the real part (n). Any errors in n are compensated by minute changes in k, which is a free parameter. In particular, the grain size and refractive index of the basalt substrate material is arbitrary, because we are only interested in the spectral reflectivity of the basalt for the specific geometry of this experiment. For any plausible n and grain size, a k can be found which results in an excellent match to the measured spectral reflectivity of the basalt substrate.

Results

We found that the behavior in the visible (400-750 nm) was well matched by models having porosity=0.9 (where 0.0 implies no gaps between dust grains), with 10 μm grains and isotropic single scattering. Smaller grain sizes required larger porosities in order to keep the optical depth of the coating layer constant. However, regardless of grain size these simple Hapke models failed to emulate the observed behavior in the near infrared (>750 nm), where reflectance falls off relative to the model for coating layers of intermediate thicknesses (Figure 1).

Because this fall-off could not be caused by a single scattering albedo effect, we hypothesized that it must be attributable to the only other Hapke parameter capable of varying with wavelength, $P(g)$. Variation of $P(g)$ with wavelength is expected for small particles with surface irregularities comparable in scale to the wavelengths of observation, and in larger particles with varying n and/or α (e.g., *Grundy et al. 2000*). Because the phase angle for

the lab measurements was fixed at 27º, we did not need to know the full phase function a priori, but could simply make $P(g=27º)$ a scalar free parameter at each wavelength. We then simultaneously fit the data for all thicknesses and wavelengths, using a variant of the SIMPLEX (*Nelder and Mead, 1965*) minimization algorithm. The result was three functions of wavelength: the absorption coefficients of the JSC-1 coating material and the basalt substrate, and $P(g)$ at g=27º. With these functions we were able to achieve an acceptable fit to the entire lab data set (Figure 2).

With $P(g)$ available only at g=27º, we could not simulate the spectrum of JSC-1 coatings at other phase angles and thus derive the full functional form of $P(g)$. However, the dependence of $P(g=27º)$ on wavelength is quite simple, decreasing monotonically with wavelength from near 1.0 at visible wavelengths to about 0.3 at 2400 nm. We note that Mie theory may provide one explanation for this effect, as it gives similar behavior over the grain size parameter range from 1-3 μm (Figure 3). However, the Mie theory amplitude is lower, which could result from the fact that Mie theory is for isolated grains, whereas our coatings consist of multiple grains in close proximity, creating additional scattering opportunities per particle. Ray optics calculations also offer an explanation for the decreasing $P(g=27º)$ with wavelength. Reductions in both n and k tend to make P(g) more forward scattering (and less scattering toward g=27º) (*Grundy et al., 2000*). Indeed, both refractive indices for palagonite diminish over the wavelength region from 1000 to 2400 nm (Figure 4). However, with our single-geometry experiment, we are unable to ascertain which mechanism is responsible for the drop in $P(g=27º)$. In future work we should be able to extend the model to arbitrary viewing and illumination geometries by using an appropriate wavelength-dependent P(g), which would be highly relevant to improving interpretation of remote-sensing observations of Mars.

Discussion and Conclusion

Plausible sets of Hapke parameters can be found that match the spectral behavior of the JSC-1 coating and basalt substrate very well. For coated samples, the two-layer Hapke model replicates the observed spectra well in the visible (400-750 nm), but overestimates the reflectance in the near-infrared, apparently because the JSC-1 particles are more forward scattering at near-infrared wavelengths than they are in the visible. This enhanced forward-scattering at infrared wavelengths is likely due to Mie scattering by JSC-1 particles that are small compared with the infrared wavelengths. The decreasing refractive indices of JSC-1 probably also contribute to increasing forward scattering with wavelength (Figures 1,4).

The observation that a pale, reddish coating applied to a dark, reddish substrate can yield a reflectance spectrum with a negative ("blue") slope calls into question the applicability of linear spectral mixture modeling of rock and coating materials in the near-infrared unless wavelength-dependent single scattering phase functions and absorption coefficients are incorporated. Figure 2 shows the data are well matched by a two-layer Hapke model that includes such a wavelength-dependent $P(g=27º)$. Further, Figure 3 shows that the wavelength dependent behavior of $P(g=27º)$ is similar to what would be predicted by a Mie scattering model. This lends credibility to our proposed explanation of the laboratory data and may provide the means

necessary to model different viewing and illumination angles of the coated samples. To confirm the validity of this approach, further laboratory studies are planned to investigate spectra of coatings as functions of illumination and emission angles.

In multiple-scattering spectral modeling of planetary surfaces, it is conventional to ignore the dependence of $P(g)$ on wavelength, and to assume that after an initial scatter or two, photons effectively "forget" their initial propagation directions, justifying the use of an isotropic (e.g., *Hapke 1993*) or simplified (e.g., *Douté and Schmitt, 1998*) single scattering phase function for all subsequent scatters. While these assumptions introduce only minor errors for deep, homogeneous media (e.g., *Cheng and Domingue, 2000*), our data point to potentially more significant problems when simulating spectral effects of thin coatings, where the wavelength-dependence of $P(g)$ can produce significant spectral signatures.

The masking effect of aeolian-deposited fine-grained coatings on rock surfaces plagues remote sensing and in-situ investigations on both the Earth and Mars from visible to thermal infrared wavelengths. Systematically combining visible/near-infrared reflectance spectra of palagonite-coated basalts and radiative transfer theory to model the results has provided an important incremental step in understanding the spectral effects of thin, fine-particle coatings. This will help clarify rock lithologies on Mars that would otherwise be obscured by dust coatings and could be useful in tracking and modeling the erosion and deposition of dust particles on the surface of Mars resulting from wind storms, dust devils (*Metzger et al., 1999; Edgett and Malin, 2000*), or mass movement activity (*Sullivan et al., 2000*). In combination with data from future Mars rover investigations into the morphology, spectroscopy, and deposition rates of atmospheric dust (e.g., *Jenkins et al., 1999*), this work also will help constrain the mineralogical identification of the dust coatings themselves.

Acknowledgments. We thank P. Lucey, J. Hinrichs, and N. Domergue-Schmidt for assistance in acquiring the visible/near-infrared reflectance spectra, T. Roush for providing optical constant data, C. Allen for the JSC-1 soil, and R. Kokaly for a Spectralon spectrum. Reviews by K. Herkenhoff, L. Gaddis and three anonymous reviewers are appreciated. WMG was supported by Hubble Fellowship grant HF-01091.01-97A. JRJ is supported by NASA PGG contract W-19,443.

References

Allen, C.C., R.V. Morris, K.M. Jager, D.C. Golden, D.J. Lindstrom, M.M. Lindstrom, J.P. Lockwood, Martian regolith simulant JSC Mars-1, *Lunar Plan. Sci. Conf. XXIX*, #1690, 1998.

Arvidson, R.E., E.A. Guinness, M.A. Dale-Bannister, J. Adams, M. Smith, P.R. Christensen, and R.B. Singer, Nature and distribution of surficial deposits in Chryse Planitia and vicinity, Mars, *J. Geophys. Res*., 94, 1573-1587, 1989a.

Arvidson, R.E., J.L. Gooding, and H.J. Moore, The Martian surface as imaged, sampled, and analyzed by the Viking landers, *Rev. Geophys.*, 27, 39-60, 1989b.

Bell III, J.F., et al., Near-infrared imaging of Mars from HST: Surface reflectance, photometric properties, and implications for MOLA data, *Icarus*, 138, 25-35, 1999.

Bell, J.F. III, et al., Mineralogic and compositional properties of Martian soil and dust: Preliminary results from Mars Pathfinder, *J. Geophys. Res.*, 105, 1721-1755, *J. Geophys. Res.*, 2000.

Cheng, A.F. and D.L. Domingue, Radiative transfer models for light scattering from planetary surfaces, *J. Geophys. Res*. 105, 9477-9482, 2000.

Christensen, P.R., Regional dust deposits on Mars: Physical properties, age, and history, *J.Geophys.Res.*, 91,3533-3545, 1986.
Christensen, P.R., et al., Thermal Emission Spectrometer experiment: Mars Observer mission, *J. Geophys. Res.*, 97, 7719-7734, 1992.
Christensen, P.R., et al., Results from the Mars Global Surveyor Thermal Emission Spectrometer, *Science*, 279, 1692-1698, 1998.
Christensen, P.R., J.L. Bandfield, M.D. Smith, V.E. Hamilton, and R.N. Clark, Identification of a basaltic component on the Martian surface from Thermal Emission Spectrometer data, *J. Geophys. Res.*, 105, 9609-9622, 2000.
Clancy, R.T., S.W. Lee, G.R. Gladstone, W.W. McMillan, and T. Roush, A new model for Mars atmospheric dust based upon analysis of ultraviolet through infrared observations from Mariner 9, Viking, and Phobos, *J. Geophys. Res*., 100, 5251-5263, 1995.
Clark, R.N, G.A. Swayze, R.B. Singer, and J.B. Pollack, High-resolution reflectance spectra of Mars in the 2.3-μm region: Evidence for the mineral scapolite, *J. Geophys. Res*., 95, 14643-14480, 1990.
Crisp, J.A., The effect of thin coatings of dust or soil on the bulk APXS composition of the underlying rocks at the Pathfinder landing site, *Lunar Planet. Sci. Conf. XXIX*, #1962, 1998.
Crisp, J., and M.J. Bartholomew, Mid-infrared spectroscopy of Pahala Ash palagonite and implications for remote sensing studies of Mars, *J. Geophys. Res.*, 97, 14691-14699, 1992.
Douté, S. and B. Schmitt, A multiplayer bidirectional reflectance model for the analysis of planetary surface hyperspectral images at visible and near-infrared wavelengths, *J. Geophys. Res*., 103, 31367-31390, 1998.
Edgett, K. S. and M. C. Malin, New views of Mars eolian activity, materials, and surface properties: Three vignettes from the Mars Global Surveyor Mars Orbiter Camera, , *J. Geophys. Res*., 105, 1623-1650, 2000.
Fischer, E.M., and C.M. Pieters, The continuum slope of Mars: Bidirectional reflectance investigations and applications to Olympus Mons, *Icarus*, 102, 185-202, 1993.
Greeley, R., N. Lancaster, S. Lee, and P. Thomas, Martian aeolian processes, sediments, and features, in *Mars*, eds. H.H. Kieffer, B.W. Jakosky, C.W. Snyder, M.W. Matthews, Univ. Arizona Press, Tucson, pp. 730-766, 1992.
Grundy, W.M., S. Douté, and B. Schmitt, A Monte Carlo ray-tracing model for scattering and polarization by large particles with complex shapes, *J. Geophys. Res*., 105, 29,291-29,314, 2000.
Hapke, B., *Theory of Reflectance and Emittance Spectroscopy*, Cambridge Univ. Press, 455 pp., 1993.
Hillier, J.K, Shadow-hiding opposition surge for a two-layer surface, Icarus, 128, 15-27, 1997.
Hiroi, T., and C.M. Pieters, Modeling the effects of surface roughness and coating on reflectance spectra, *Trans. Amer. Geophys. Union*, 73, 187, 1992.
James, P.B., J.L. Hollingsworth, M.J. Wolff, and S.W. Lee, North polar dust storms in early spring on Mars,*Icarus*,138,64-73, 1999.
Jenkins, P.P., et al., Status of the dust accumulation and removal technology experiment for the Mars 2001 Surveyor lander, in *The Fifth International Conference on Mars*, #6203, LPI Contribution No. 972, Lunar and Planetary Institute, Houston (CD-ROM), 1999.
Johnson, J.R., P.R. Christensen, and P.G. Lucey, Dust coatings on basalts and implications for thermal infrared spectroscopy of Mars, *J. Geophys. Res*., submitted, 2000.
Johnson, J.R., P.G. Lucey, K.A. Horton, and E.M. Winter, Infrared measurements of pristine and disturbed soils 1. Spectral contrast differences between field and laboratory data, *Rem. Sens. Environ*., 64, 34-46, 1998.
Kieffer, H.H., B.M. Jakosky, C.W. Snyder, The planet Mars: From antiquity to the present, in *Mars*, eds. H.H. Kieffer, B.W. Jakosky, C.W. Snyder, M.W. Matthews, Univ. Arizona Press, Tucson, pp. 1-33, 1992.
Landis, G.A., and P.P. Jenkins, Measurement of the settling rate of atmospheric dust on Mars by the MAE instrument on Mars Pathfinder, , *J. Geophys. Res*., 105, 1855-1857, 2000.
Martin, L.J., and R.W. Zurek, An analysis of the history of dust activity on Mars, *J. Geophys. Res.*, 98, 3221-3246, 1993.

McSween, H.Y., Jr., et al., Chemical, multispectral, and textural constraints on the composition and origin of rocks at the Mars Pathfinder landing site, *J. Geophys. Res.*, 104, 8679-8716, 1999.

Metzger, S.M., J.R. Carr, J.R. Johnson, T.J. Parker, and M. Lemmon, Dust devil vortices seen by the Mars Pathfinder camera, *Geophys. Res. Lett.*, 26 , No. 18 , 2781-2784, 1999.

Mustard, J.F., and J.M. Sunshine, Seeing through the dust: Martian crustal heterogeneity and links to the SNC meteorites, *Science*, 267, 1623-1626, 1995.

Mustard, J.F., and J.E. Hays, Effects of hyperfine-particles on reflectance spectra from 0.3 to 25μm, *Icarus*,125, 145-163, 1997.

Mustard, J.F., et al., The surface of Syrtis Major: Composition of the volcanic substrate and mixing with altered dust and soil, , *J. Geophys. Res*., 98, 3387-3400, 1993.

Nelder, J. and R.Mead, A simplex method for function minimization, *Computer J.*, 7, 308-313, 1965**.**

Pollack, J.B., D.S. Colburn, F.M. Flasar, R. Kahn, C.E., Carlston, and D.C. Pidek, Properties and effects of dust particles suspended in the Martian atmosphere, *J. Geophys. Res.*,84,2929-2945, 1979.

Rieder, R., et al., The chemical composition of martian soil and rocks returned by the mobile Alpha Proton X-Ray spectrometer: Preliminary results from the X-ray mode, *Science*, 278, 1771-1774, 1997.

Roush, T.L., Effects of iron-silica gels on spectral reflectance, *Lunar Plan. Sci. Conf. XIII*, 661-662,1982.

Salisbury, J.W., *Spectral Measurements Field Guide*, Defense Technology Information Center, Rpt. No. ADA362372, 1998.

Singer, R.B., and T.L. Roush, Spectral reflectance properties of particulate weathered coatings on rocks: Laboratory modeling and applicability to Mars, *Lunar Plan. Sci. Conf. XIV*, 708-709, 1983.

Sullivan, R., K. Edgett, M. Malin, P. Thomas, and J. Veverka, Mass-wasting slope streaks imaged by the Mars Orbiter Camera**,** *Lunar Plan. Sci. Conf. XXXI*, #1911, 2000.

Thomas, P.C., J. Veverka, D. Gineris, and L. Wong, "Dust" streaks on Mars, *Icarus*, 60, 161-179, 1984.

Thomas, P.C., M.C. Malin, M.H. Carr, G.E. Danielson, M.E. Davies, W.K. Hartmann, A.P. Ingersoll, P.B. James, A.S. McEwen, L.A. Soderblom, and J. Veverka, Bright dunes on Mars, *Nature*, 397, 592-594, 1999.

Tomasko, M.G., L.R. Doose, M. Lemmon, P.H. Smith, and E. Wegryn, Properties of dust in the Martian atmosphere from the Imager on Mars Pathfinder, *J.Geophys.Res*.,104,8987-9008,1999.

Wells, E.N., J. Veverka, and P. Thomas, Mars: Experimental study of albedo changes caused by dust fallout,*Icarus*,58,331-338,1984.

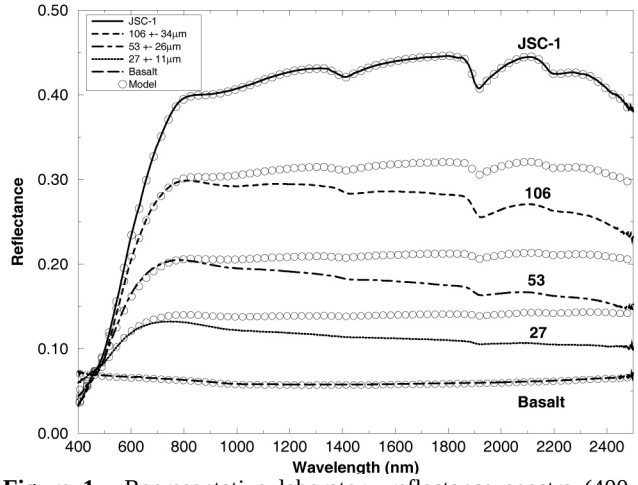

Figure 1. Representative laboratory reflectance spectra (400-2500 nm) of SP basalt with different coating thicknesses (in microns) of JSC-1. Spectra are compared to fits of Hapke model (circles, with modeled thickness labeled) assuming isotropic single scattering.

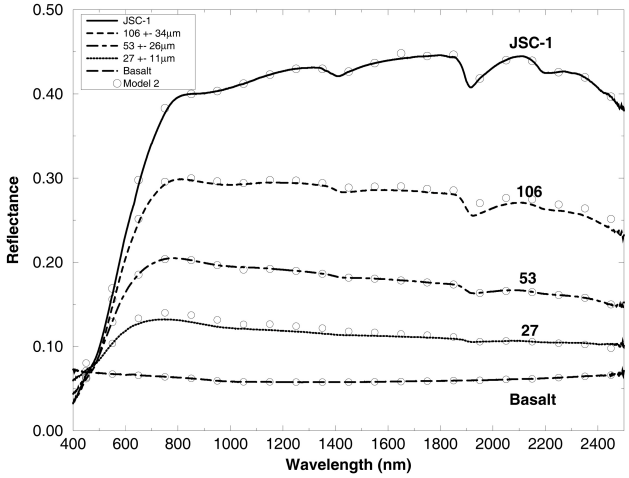

Figure 2. Lab spectra and revised Hapke fit (circles) in which $P(g=27^{o})$ and the absorption coefficients were varied separately to minimize errors for the entire data set. Grain sizes and porosity were the same as Figure 1 (see text).

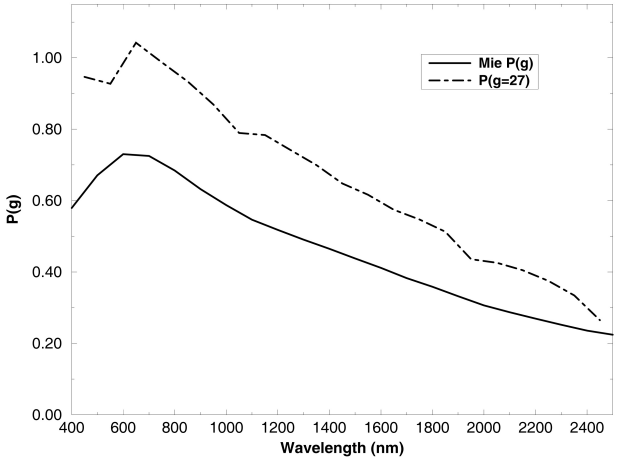

Figure 3. Comparison of fitted $P(g=27^{o})$ phase function and a compound Mie phase function composed of the sum of Mie functions for grain sizes D=1.1±50% µm and D=2.4±50% µm, weighted 0.65 and 0.35, respectively.

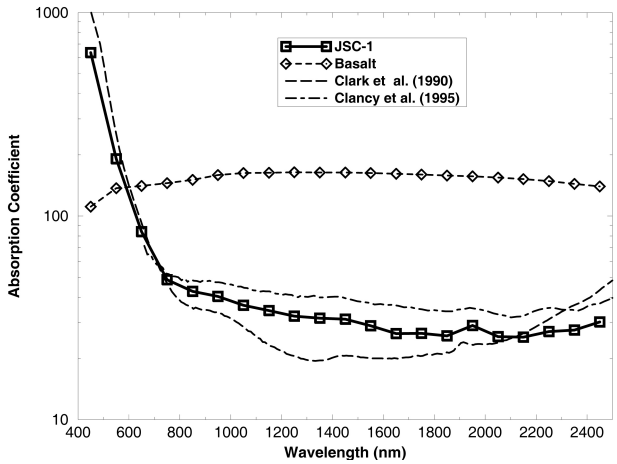

Figure 4. Derived absorption coefficients for JSC-1 (and basalt) compared to those derived for palagonites from *Clark et al. (1990)* and *Clancy et al. (1995).*